Mon. Not. R. Astron. Soc. **301,** 1083–1094 (1998)

Silicate and hydrocarbon emission from Galactic M supergiants

R. J. Sylvester,[1] C. J. Skinner[2] and M. J. Barlow[1]
[1]*Department of Physics and Astronomy, University College London, Gower Street, London WC1E 6BT*
[2]*Space Telescope Science Institute, 3700 San Martin Drive, Baltimore, MD 21218, USA*

Accepted 1998 August 18. Received 1998 August 14; in original form 1998 June 15

ABSTRACT

Following our discovery of unidentified infrared (UIR) band emission in a number of M supergiants in h and χ Per, we have obtained 10-μm spectra of a sample of 60 galactic M supergiants. Only three new sources, V1749 Cyg, UW Aql and IRC+40 427, appear to show the UIR bands; the others show the expected silicate emission or a featureless continuum. The occurrence of UIR-band emission in M supergiants is therefore much higher in the h and χ Per cluster than in the Galaxy as a whole. Possible explanations for the origin and distribution of UIR bands in oxygen-rich supergiants are discussed. We use our spectra to derive mass-loss rates ranging from 10^{-8} to 10^{-4} $M_{\odot}$ yr^{-1} for the new sample, based on the power emitted in the silicate feature. The relationship between mass-loss rate and luminosity for M supergiants is discussed, and correlations are explored between their mid-infrared emission properties.

Key words: circumstellar matter – stars: mass-loss – supergiants – open clusters and associations: individual: h and χ Per – infrared: stars.

1 INTRODUCTION

M supergiants are massive evolved stars with high luminosities ($L > 5 \times 10^4$ $L_{\odot}$) and low surface temperatures ($T_{\rm eff} \sim 3000$ K). They undergo significant mass loss, which can be evident from blueshifted optical absorption lines, submillimetre CO emission and excess infrared (IR) emission caused by circumstellar dust. Standard equilibrium chemistry (e.g. Gilman 1969) predicts that the less abundant of the elements carbon and oxygen will be entirely bound up in the highly stable form of CO molecules. In consequence, the dust that forms around oxygen-rich (C/O < 1) stars should be composed only of oxygen-rich materials, e.g. silicates and oxides, while carbon-rich stars (C/O > 1) should produce only carbon-rich dust, such as SiC, graphite, etc.

This scenario is generally supported by observations, although some exceptions have been found. A number of J-type carbon stars show silicate emission in their *IRAS* LRS spectra (Willems & de Jong 1986; Skinner, Griffin & Whitmore 1990; Lloyd Evans 1990; Kwok & Chan 1993).

Two oxygen-rich M supergiants, MZ Cas and AD Per, were found by Skinner & Whitmore (1988a, hereafter SW) to show an emission peak at ~11.5 μm, which those authors attributed to SiC. We obtained ground-based mid-IR spectra of both these stars, and of 14 other M supergiants in the h and χ Per association (Sylvester, Barlow & Skinner 1994, hereafter Paper 1), and found that MZ Cas, AD Per and five other sources showed emission features at 11.3 and 8.7 μm, the so-called unidentified infrared (UIR) bands, attributed to carbonaceous species such as polycyclic aromatic hydrocarbons (PAH). These bands were superposed on broad silicate features, which peaked at around 10.5 μm, while many of the stars without UIR bands show strong silicate features peaking closer to 9.7 μm, a peak wavelength more usual for circumstellar silicates.

We explained the presence of the UIR bands in terms of the non-equilibrium chemistry models of Beck et al. (1992), where ultraviolet (UV) photons from a warm chromosphere dissociate CO molecules, providing free C atoms from which carbonaceous PAH-like species can form. The UV radiation also provides the energy to excite UIR-band emission.

We were able to distinguish the UIR bands in MZ Cas and AD Per because the resolving power of CGS3 (Section 2) is higher than that of the *IRAS* LRS. Similarly, the other UIR-emitting supergiants have rather noisy LRS spectra, and hence were not noted as being unusual, but the higher sensitivity of CGS3 allowed us to detect the bands. We have therefore undertaken a new CGS3 observational survey of a large sample of Galactic M supergiants (plus a few late K-type supergiants) in order to determine how common UIR-band emission is among cool oxygen-rich supergiants, and to determine mass-loss rates for a larger sample than that of SW.

2 OBSERVATIONS

All our observations were made at UKIRT, using the Cooled Grating Spectrometer 3 (CGS3), a common-user instrument designed and built at University College London. The majority of the spectra were obtained on 1995 August 16 and 17, with a few spectra being taken during other observing runs. We used the low-resolution 10-μm grating, which gave a spectral resolution of 0.17 μm, and a wavelength coverage of 7.5–13.3 μm. The beam size used was 5.5 arcsec. Wavelength calibration was with respect to a Kr arc lamp. For each source, two subspectra were taken with

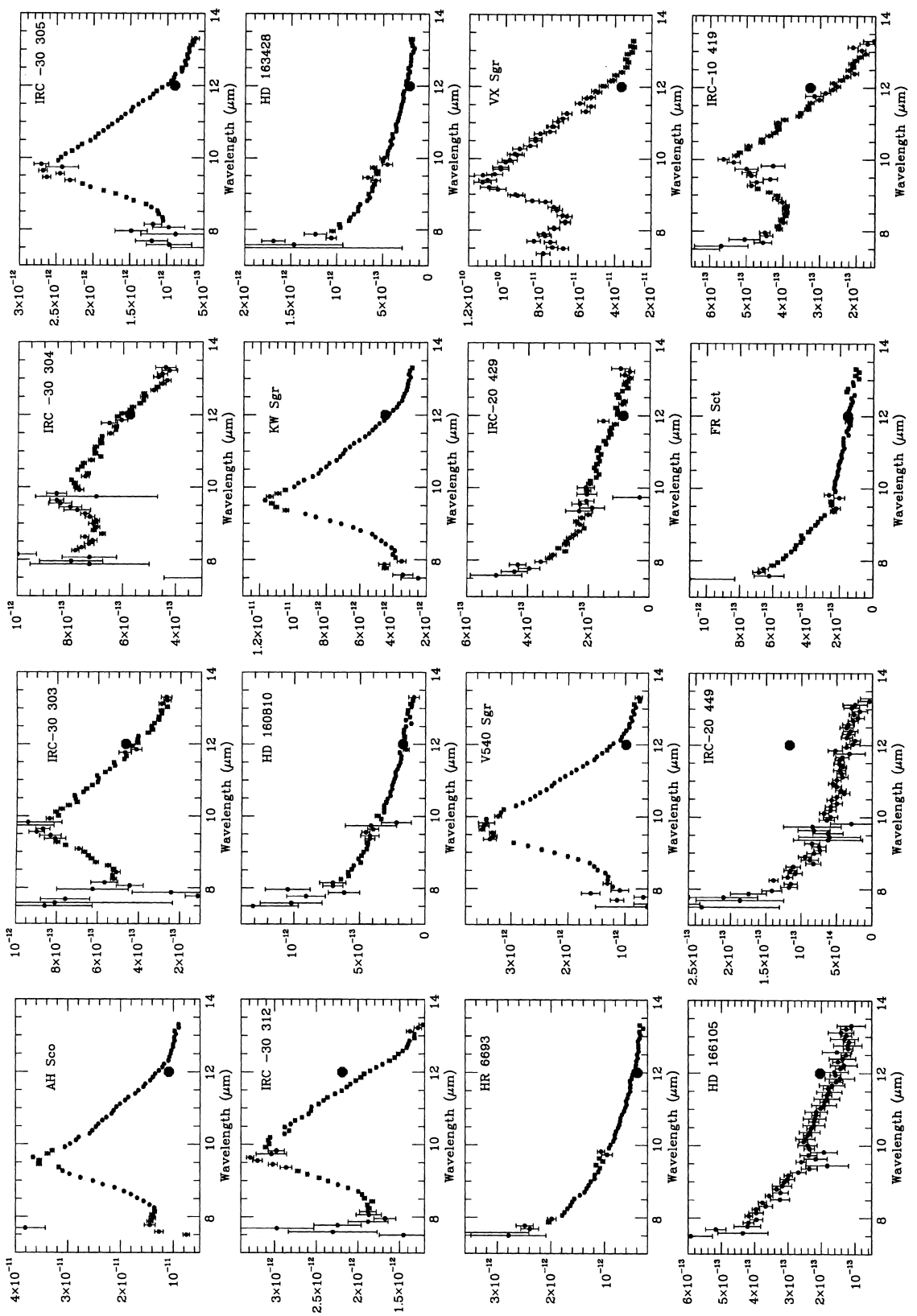

Figure 1. CGS3 spectra of M supergiants. The filled circles are colour-corrected *IRAS* 12-μm fluxes. Flux units are W m^{-2} μm^{-1}. Most of the stars show silicate emission, while UW Aql, V1449 Cyg and IRC+40 427 also show the UIR bands.

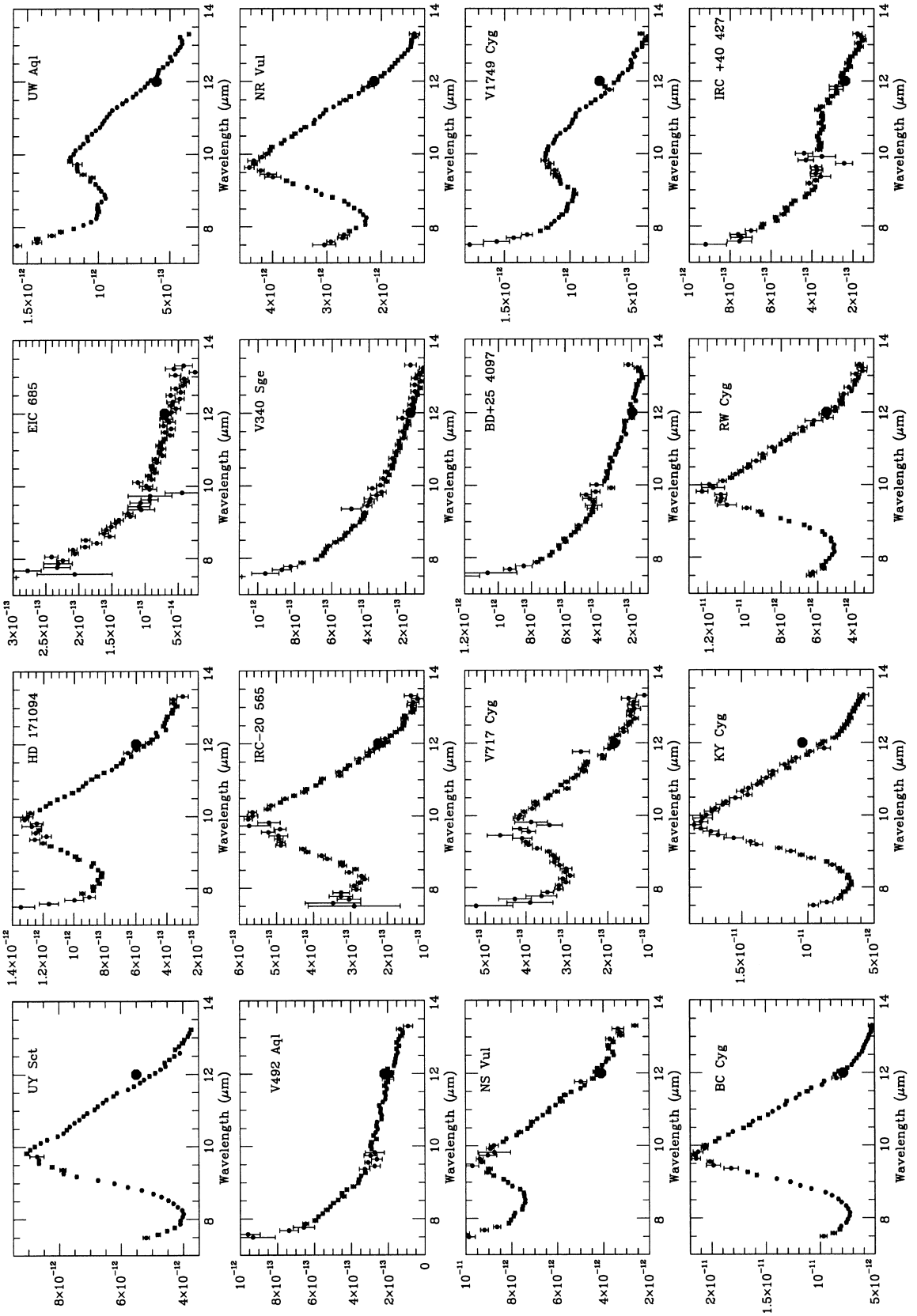

Figure 1 – *continued*

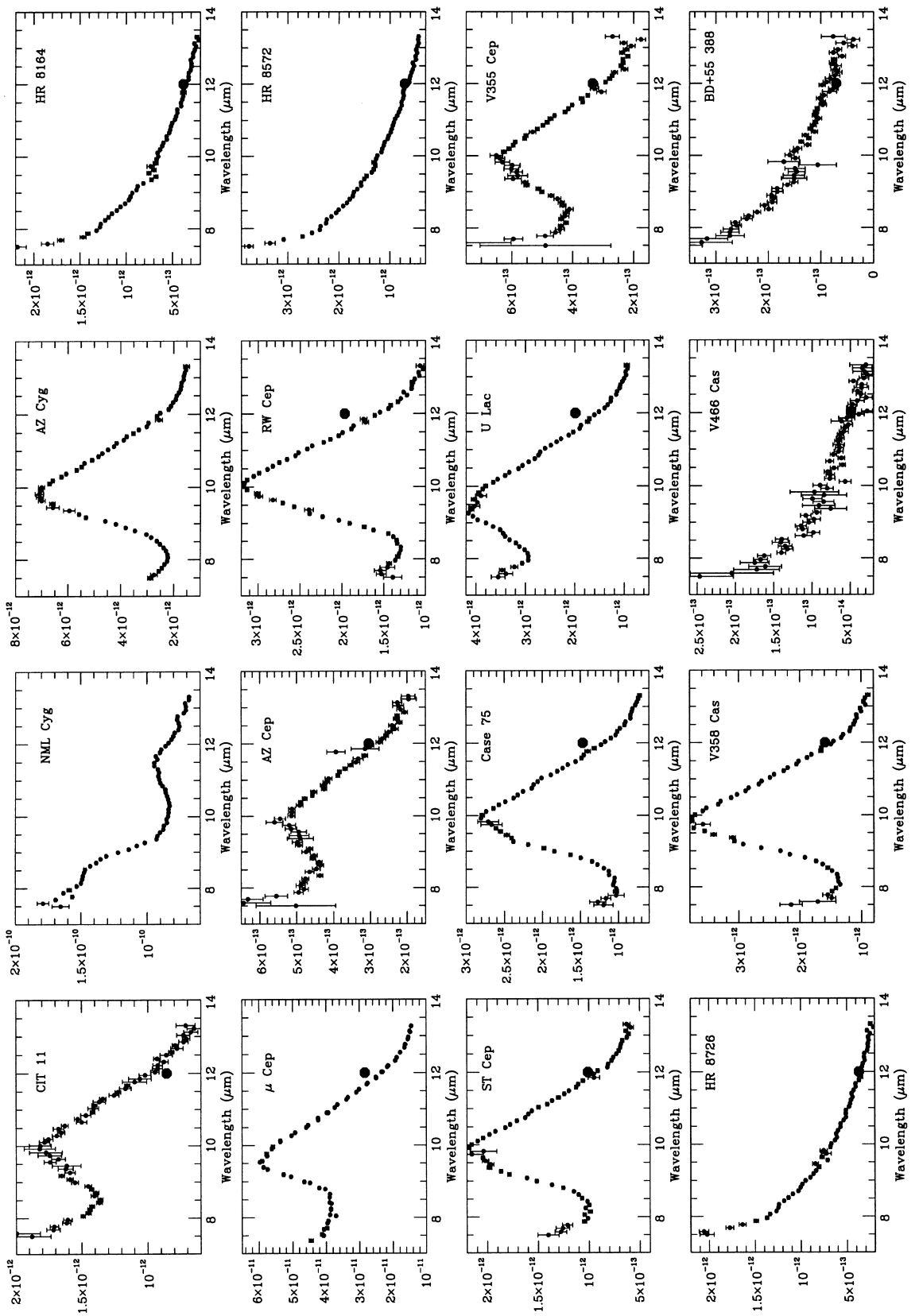

Figure 1 – *continued*

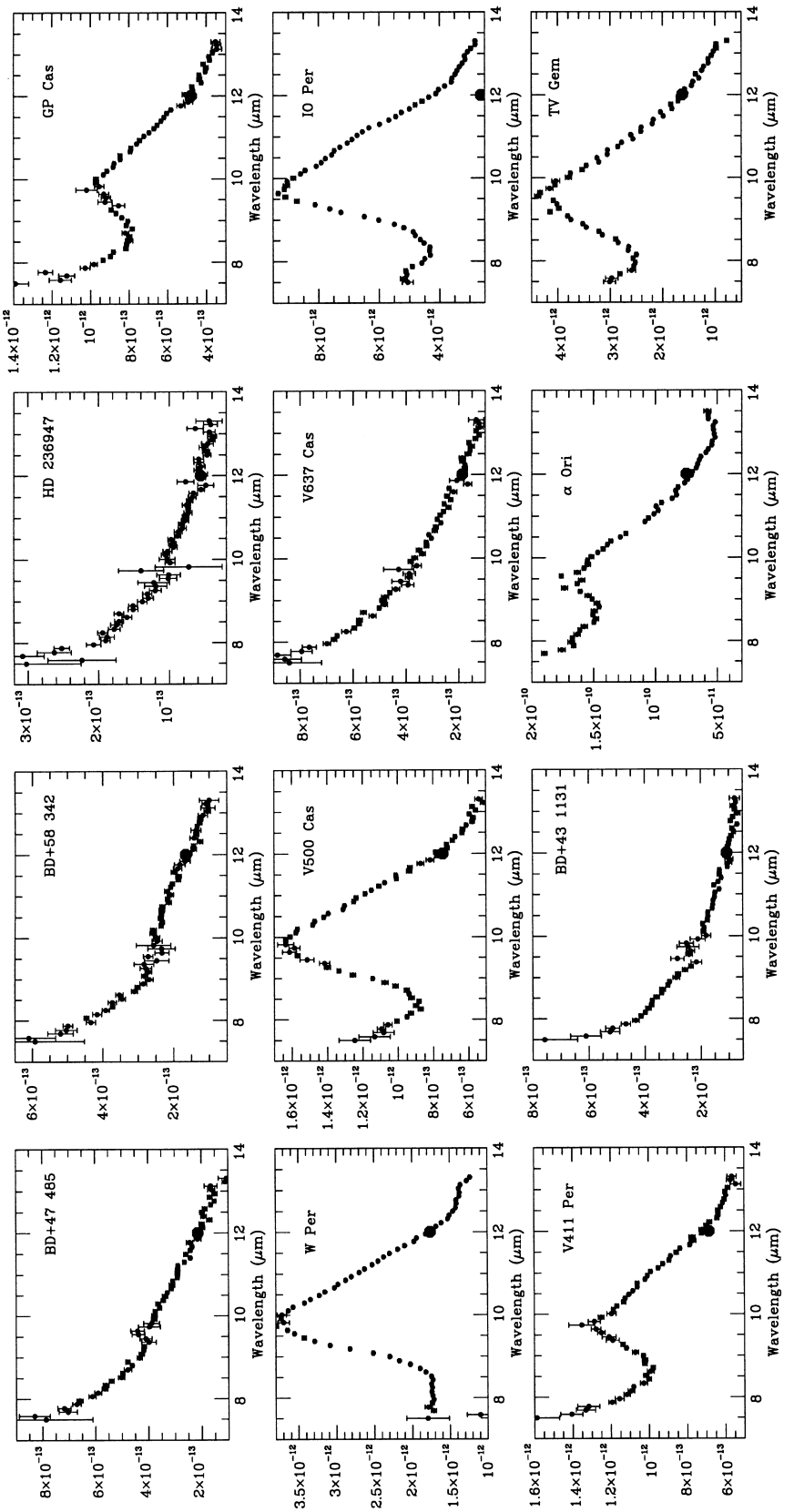

Figure 1 – *continued*

Table 1. The observed stars, listed in RA order starting from 17 h. Columns include the date of observation (1995 August unless specified), the adopted standard star, *IRAS* 12-μm flux, estimated distance, silicate feature strength ($B_{\rm sil}$), mass-loss rate, and the peak wavelength and full width at half-maximum of the silicate feature. See Section 4 for the sources of spectral types and distances, and discussion of $B_{\rm sil}$ and $\dot{M}$. AZ Cyg and NML Cyg are in a region that was not fully scanned by *IRAS*, and hence have no PSC data.

Star	*IRAS* name	Spectral type	Date	Standard	F_{12} (Jy)	Dist (kpc)	$B_{\rm sil}$	$\dot{M}$ ($M_\odot$ yr^{-1})	$\lambda_{\rm peak}$ (μm)	FWHM (μm)
AH Sco	17080−3215	M5Ia-Iab	16	η Sgr	630	4.6	10.3	4.5×10^{-4}	9.6	2.4
IRC−30 303	17322−3159	M2Iab	16	σ Lib	24	2.5	7.6	3.7×10^{-6}	9.7	2.4
IRC−30 304	17336−3213	M3Ia$^-$	16	η Sgr	25	4.2	3.1	3.9×10^{-6}	∼10.5	>4
IRC−30 305	17348−3207	M3.3Ib	17	σ Lib	50	1.8	10.9	5.6×10^{-6}	9.8	2.6
IRC−30 312	17374−3156	M2.6Ia$^-$	16	η Sgr	102	2.0	6.8	8.8×10^{-6}	10.1	3.5
HD 160810	17400−3516	M0.7Ib	16	η Sgr	11	1.3	1.4	6.1×10^{-8}	–	–
KW Sgr	17488−2800	M2.4Ia	16	η Sgr	250	3.0	10.9	7.8×10^{-5}	9.6	2.3
HD 163428	17540−2356	M0.6Iab$^-$	16	η Sgr	15	1.6	−0.1	$<4.5\times10^{-8}$	–	–
HR 6693	17558−3014	M1.2Ib$^-$	17	η Sgr	26	0.7	0.4	$<1.5\times10^{-8}$	–	–
V540 Sgr	17566−3555	M5Iab	16	η Sgr	57	3.5	11.6	2.7×10^{-5}	9.7	2.4
IRC−20 429	18045−1918	M2Iab−Ib	16	η Sgr	6.0	1.5	0.6	5.4×10^{-9}	10.6	2.8
VX Sgr	18050−2213	M4Ia	7/5/91	α Boo	2738	1.7	6.6	1.6×10^{-4}	9.4	2.9
HD 166105	18068−1517	M1Iab	16	γ Aql	13	2.0	0.5	$<6.3\times10^{-8}$	–	–
IRC−20 449	18107−1914	M2.0Ib	16	η Sgr	7.7	3.5	0.4	$<1.1\times10^{-7}$	–	–
FR Sct	18205−1242	M2.2Iab$^-$	17	γ Aql	10	2.6	−1.8	$<8.2\times10^{-8}$	–	–
IRC−10 419	18227−1347	M2.5Iab	17	γ Aql	18	2.2	5.4	1.5×10^{-6}	10.0	2.7
UY Sct	18248−1229	M3.4Ia	27/6/98	γ Aql	259	2.9	8.3	5.8×10^{-5}	9.9	3.6
HD 171094	18305−1408	M3.0Iab	17	γ Aql	35	2.1	8.0	3.9×10^{-6}	10.0	2.6
EIC 685	18336−0855	M3.5(I)	17	γ Aql	4.2	4.6	−1.8	$<1.1\times10^{-7}$	–	–
UW Aql	18550+0023	M2.2Iab	27/6/98	γ Aql	30	2.0	4.6	1.7×10^{-6}	10.1	3.0
V492 Aql	18569+0518	M1.1Iab	17	γ Aql	12	2.3	−1.1	$<7.8\times10^{-8}$	–	–
IRC−20 565	19272−1929	M2Ib	17	γ Aql	14	2.5	9.6	2.8×10^{-6}	9.9	2.4
V340 Sge	19371+1627	K5.5Iab	16	γ Aql	12	1.1	0.4	$<1.7\times10^{-8}$	–	–
NR Vul	19480+2447	M1.1Ia	16	γ Aql	106	2.5	7.8	1.7×10^{-5}	9.7	3.1
NS Vul	19503+2219	M2:(I)+B	17	ε Cyg	278	0.6	4.8	1.2×10^{-6}	9.5	2.9
V717 Cyg	19590+3041	M2.8Iab	17	ε Cyg	11	3.2	5.6	1.9×10^{-6}	10.0	2.6
BD+25 4097	20037+2527	M3−Ib	16	γ Aql	13	0.4	0.7	1.7×10^{-9}	10.4	3.4
V1749 Cyg	20193+3527	M2.6Iab	17	β Peg	42	1.8	4.2	1.7×10^{-6}	10.2	3.1
BC Cyg	20197+3722	M3.2Iab	16	γ Aql	424	1.8	11.9	5.3×10^{-5}	9.7	2.5
KY Cyg	20241+3811	M3.9Iab	16	γ Aql	511	1.8	10.2	5.5×10^{-5}	9.7	2.7
RW Cyg	20270+3948	M2.9Iab	16	ε Cyg	298	1.0	8.9	8.6×10^{-6}	9.9	2.8
IRC+40 427	20296+4028	M0−2I	16	ε Cyg	13	2.0	−0.3	$<6.3\times10^{-8}$	11.2	2.8
CIT 11	20377+3901	M4(Ia)	16	ε Cyg	45	2.5	4.5	3.9×10^{-6}	10.1	3.8
NML Cyg	20445+3956	M6	7/10/92	β Peg	–	2.0	(abs)	–	–	–
AZ Cyg	($20^{\rm h}56^{\rm m}$)	M3.1Iab	16	γ Aql	–	2.9	13.8	5.2×10^{-5}	9.8	2.4
HR 8164	21178+5824	M1.1Ib	17	β Peg	24	1.0	0.5	$<2.7\times10^{-8}$	–	–
μ Cep	21419+5832	M2.2Ia	24/5/91	β Peg	1296	0.8	7.9	2.3×10^{-5}	9.6	2.7
AZ Cep	22069+5918	M1.6Ia	16	β Peg	16	1.0	4.1	2.0×10^{-7}	10.2	3.3
RW Cep	22212+5542	K5: Ia−0	16	β Peg	97	2.8	7.5	1.8×10^{-5}	10.1	2.8
HR 8572	22274+4726	M0.3Iab	17	β Peg	47	0.5	0.7	9.4×10^{-9}	–	–
ST Cep	22282+5644	M2.6Ia	17	β Peg	55	1.0	9.4	1.7×10^{-6}	9.9	2.6
Case 75	22317+5838	M2.7Iab	17	β Peg	78	2.8	11.1	2.2×10^{-5}	9.9	2.7
U Lac	22456+5453	M2.5Ia	17	β Peg	124	2.8	7.4	2.3×10^{-5}	9.8	2.7
V355 Cep	22471+5902	M1.1Iab	16	β Peg	19	2.8	6.4	3.0×10^{-6}	10.0	2.6
HR 8726	22542+4927	K5.8Ib	17	β Peg	25	0.6	0.5	$<9.9\times10^{-9}$	–	–
V358 Cas	23281+5742	M2.8Ia	16	β And	84	3.2	11.4	3.2×10^{-5}	9.9	2.5
V466 Cas	01167+5802	M1.1Ib	17	β Peg	2.9	2.5	0.6	1.2×10^{-8}	–	–
V595 Cas	01397+5615	M3.7Ib	16	β And	4.7	2.8	0.0	$<4.4\times10^{-8}$	–	–
BD+47 485	01400+4815	M2Ib	16	β And	12	1.5	0.9	3.3×10^{-8}	10.3	3.4
BD+58 342	01550+5901	M2.4Ib	16	β And	8.9	2.3	0.0	$<5.7\times10^{-8}$	11.0	3.2
HD 236947	02036+5832	M0.6Ib	17	β Peg	3.9	2.3	−0.3	$<2.5\times10^{-8}$	–	–
GP Cas	02360+5922	M2.8Iab	16	β And	26	2.3	3.9	1.6×10^{-6}	10.0	3.0
W Per	02469+5646	M3.6Iab	4/10/92	α Tau	90	4.3	9.1	4.9×10^{-5}	9.9	2.8
V500 Cas	02473+5738	M2.9Iab	16	β And	39	2.3	7.1	4.6×10^{-6}	9.9	2.8
V637 Cas	02531+5721	M2.2Iab$^-$	16	β And	12	1.9	0.4	$<5.1\times10^{-8}$	–	–
IO Per	03030+5532	M3.9Iab$^-$	17	α Aur	240	1.9	8.9	2.5×10^{-5}	9.8	2.8
V411 Per	03113+5441	M3.4Ia$^-$	17	α Aur	36	2.2	4.0	2.1×10^{-6}	9.8	>4
BD+43 1131	04524+4324	M2Ib	17	β Peg	7.0	0.3	0.2	$<7.6\times10^{-10}$	–	–
α Ori	05524+0723	M2.2Iab$^-$	1/11/93	α CMa	4682	0.2	3.7	2.1×10^{-6}	9.9	2.6
TV Gem	06088+2152	M0.6Iab	17	α Aur	96	1.5	8.9	6.2×10^{-6}	9.8	2.7

the grating positions displaced by half a resolution element. The subspectra were then interleaved in the data reduction process to produce a fully sampled 64-point spectrum. Because the two subspectra are not taken simultaneously, changes in e.g. the atmospheric transmission can give rise to differences in the spectral shape or signal-to-noise ratio between the two subspectra. Such artefacts are apparent in the spectrum of HD 166105 presented in Fig. 1. The telescope secondary mirror was chopped east–west at 5 Hz with a 30-arcsec throw. Sky spectra taken using a rotating sector chopper were used for flat-fielding all spectra.

Flux calibration was achieved by ratioing the target star with the observed spectrum of a standard star, and multiplying by the absolutely calibrated spectra compiled by Cohen & Davies (1995) and Cohen, Walker & Witteborn (1992), or by blackbodies in the case of the observations made in 1991. Further details of the instrument (and its role in IR spectral calibration) are given by Cohen & Davies (1995).

Our α Ori spectrum (taken with the 5.5-arcsec aperture) probably underestimates the total flux from the source, because the dust emission from α Ori is known to be spatially extended over several arcseconds (Sloan, Grasdalen & LeVan 1993).

Our target stars, the dates of the observations and the standard stars used are listed in Table 1. We also include the *IRAS* names of the associated IR sources. Our sources mostly lie within a few degrees of the Galactic plane, and span the range 350°–150° in Galactic longitude.

Five stars in the present paper (V500 Cas, BD+58 342, HD 236947, GP Cas and W Per) are possible members of the Per OB1 association, which contains h and χ Per, and should probably be considered as h and χ Per supergiants. However, the distance found by Humphreys (1970) for W Per is 4.3 kpc, whereas h and χ Per are approximately 2.3 kpc away (Humphreys 1978).

3 THE SPECTRA

The observed spectra are presented in Fig. 1, along with the *IRAS* 12-μm Point Source Catalog (PSC) fluxes. The *IRAS* data were colour-corrected using the shape of the CGS3 spectra and the published *IRAS* 12-μm filter profile. Agreement between the two data sets is good: for more than 40 of the 58 stars with *IRAS* data, the CGS3 and PSC fluxes agree to within approximately 10 per cent. This implies both that the photometric calibration of the CGS3 spectra is good, and that M supergiants, despite often being optically variable, do not tend to vary strongly in the 10-μm region. The latter point is in agreement with Monnier, Geballe & Danchi (1998), who found that α Ori and α Sco both showed little variability at 10 μm, and no variation in silicate feature strength, unlike many Mira stars. Similarly, Bester et al. (1996) found that in the period 1988–1995, α Ori varied by $\sim$0.15 mag at 11.15 μm, but by $\sim$0.7 mag at V. Examining the variability measure, VAR, in the *IRAS* PSC data for our targets, we find that only five of 56 show evidence of IR flux variability with amplitude $\gtrsim$10 per cent, and only VX Sgr appeared to vary with an amplitude $\gtrsim$ 20 per cent. In all cases, the 12-μm fluxes in Fig. 1 and Table 1 are the average PSC fluxes.

In the longer-wavelength *IRAS* bands, BC Cyg is confused with another source (Jura & Kleinmann 1990), but the good agreement between the CGS3 and *IRAS* 12-μm fluxes suggests that the PSC 12-μm measurement is not contaminated by flux from the nearby source, since the CGS3 beam is much smaller than that of *IRAS*.

Of the 15 stars where a significant discrepancy exists, 11 have lower fluxes in the CGS3 spectra than in the PSC data, while only four are brighter in the CGS3 spectra. This imbalance suggests that the discrepancies may result from observational effects (thin cloud, slight pointing errors) as well as from intrinsic variability.

The error bars tend to be larger around 9.5 μm, owing to absorption by telluric ozone, and shortwards of about 8 μm, owing to water vapour absorption. As well as contributing noise, these strong absorptions do not always cancel out completely when ratioing the spectrum of a target star to that of a standard star, which can cause spurious features to appear in the spectra.

Many of the spectra show some curvature around 8 μm; this is the result of absorption in the SiO fundamental band. SiO absorption in the fundamental and first overtone bands is common in late-type stars (e.g. Rinsland & Wing 1982; Cohen & Davies 1995). Detection of the 8-μm SiO fundamental in our spectra is complicated by the fact that many of the late-type standard stars we used also show SiO absorption (Cohen & Davies 1995). Repeating the data reduction using earlier-type standards, e.g. α Aur, that do not have SiO bands, showed that the features are indeed intrinsic to our sources and not an artefact of the data reduction.

Inspection of Fig. 1 reveals that the majority of the supergiant spectra (35 of 60 sources) show strong silicate emission features without noticeable UIR-band emission. Most of the remaining sources show seemingly featureless spectra, while NML Cyg shows silicate self-absorption. There is a wide range in silicate feature strength relative to the mid-IR continuum, which is reflected in the range of values of the silicate strength parameter, $B_{\rm sil}$ (see below), presented in Table 1.

The present sample clearly differs from the h and χ Per M supergiants, where one-third of the sample showed the UIR bands very clearly in their spectra. Several of the stars with strong silicate features show an inflection at around 11 μm (e.g. IO Per, KW Sgr and NR Vul; see Fig. 1), but without corroborating detections of other bands we are reluctant to ascribe the 11-μm inflections to UIRs; they could be spurious, or even be the crystalline silicate features such as those which *ISO* SWS spectra have shown to be present in many objects (see e.g. Waters et al. 1996).

UIR-band emission is, however, unambiguously detected in the spectrum of V1749 Cyg. This M2.6Iab star lies in the Cygnus OB1 association (Humphreys 1978), and so is the first M supergiant outside the Perseus–Cassiopeia region found to show the UIR features. With an *IRAS* 12-μm flux of 42 Jy, it is also substantially brighter than the Per–Cas supergiants with UIR bands.

Fig. 2 shows the V1749 Cyg spectrum after subtraction of a 'photospheric' 3300-K blackbody, normalized to the observed spectrum at 8 μm. The blackbody temperature was derived from the spectral type, using the calibration of Schmidt-Kaler (1982). Also plotted is the blackbody-subtracted spectrum of RW Cep, normalized to the V1749 Cyg spectrum at 10 μm. RW Cep was selected from our sample because its silicate feature, like that of V1749 Cyg, peaks close to 10.0 μm, whereas most of the supergiant silicate features peak at the canonical 9.8 μm. The spectral type of RW Cep is K5I, the earliest of our entire sample. RW Cep shows no UIR features, and comparison of the two CGS3 spectra emphasizes the presence of the bands in V1749 Cyg. Strong bands are seen at 11.2 and 10.5 μm, along with a weaker 8.6-μm band. The 12.7-μm band may also be present, but the scatter in this region of the spectrum is rather large. The 10.5-μm feature is not one of the standard suite of UIR bands, but was present in many of the h and χ Per UIR sources (Paper 1), and coincides with a band in the spectra of several PAHs (see e.g. fig. 1 of Allamandola, Tielens & Barker 1989). The rise shortward of 8 μm might include a contribution

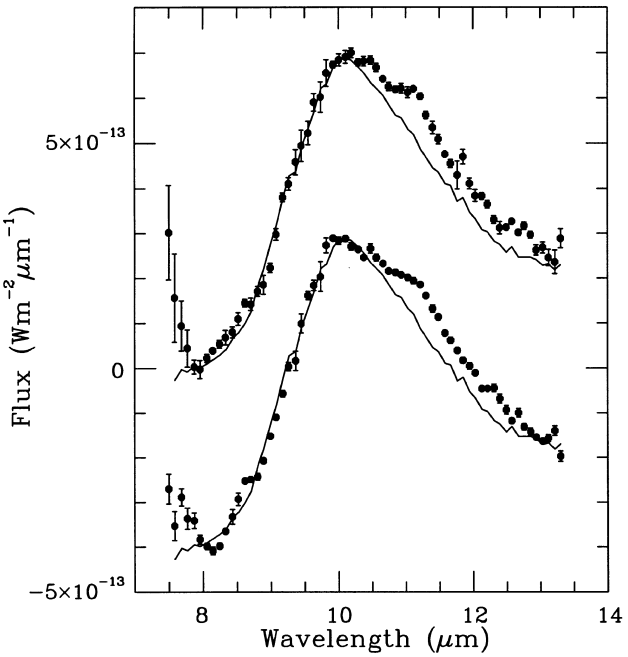

Figure 2. Blackbody-subtracted spectra of V1749 Cyg (upper points) and UW Aql (lower points), which have been shifted along the vertical axis. The blackbody-subtracted spectrum of RW Cep, normalized at 10 μm, is shown (solid lines) for comparison.

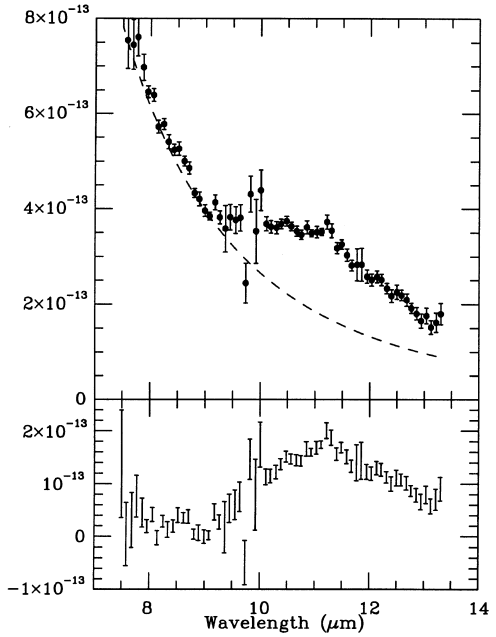

Figure 3. Upper panel: observed spectrum of IRC+40 427, with a 'photospheric' 3550-K blackbody. Lower panel: the blackbody-subtracted spectrum.

from the 7.7-μm UIR band, but could also be caused by poor cancellation of telluric water vapour absorption.

UW Aql also shows the UIR bands. The spectrum of this source is strikingly similar to that of V1749 Cyg, as can be seen in Fig. 2. Although the *IRAS* flux of V1749 Cyg is 40 per cent higher than that of UW Aql, their mid-IR fluxes as measured by CGS3 in 1995 August and 1998 June respectively differ by only a few per cent. Again, comparison with the spectrum of RW Cep enhances the visibility of the bands. The 8.6- and 11.3-μm bands are clearly present. The apparent peaks at 10.5 and 12.3 μm are probably not real features, but results of contamination by telluric absorption.

The spectrum of IRC+40 427 is very similar to those of the h and χ Per supergiants with UIR bands, for example FZ Per (see fig. 1 of Paper 1). In Fig. 3 we present the observed and blackbody-subtracted spectra of IRC+40 427. The 11.3-μm band is clearly present, along with probable 8.6- and 10.5-μm features. The broad underlying dust feature seems to peak nearer to 11 than to 10 μm, so there could in principle be a contribution from SiC dust emission. However, we do not see any structure at 10.6 and 12.4 μm corresponding to the longitudinal and transverse phonon modes (Treffers & Cohen 1974). The *IRAS* LRS spectrum of this source shows the 18-μm silicate feature, so the 10–11 μm feature must be at least partly caused by silicate emission. We note that the M supergiants MZ Cas and AD Per were thought by SW to show SiC emission since their LRS spectra are classified as type 4, but in reality they are UIR-emission sources. In Paper 1, we showed that the silicate features of the UIR-emitting supergiants peaked at longer wavelengths than those of the 'normal' M supergiants (see discussion below): IRC+40 427 seems to be an extreme example of this phenomenon.

The spectra of four of the remaining stars, GP Cas, V717 Cyg, CIT 11 and IRC−10 419, show structure close to 11.3 μm. For GP Cas, the possible features appear as breaks in the spectra rather than emission peaks, and hence are unlikely to be UIR emission. The other three spectra are rather noisy, and it is difficult to determine whether the 11-μm features are genuine UIR bands or arise from noise or calibration problems. We note that there is no correlation between the presence of these bumps and the choice of standard star used in the data reduction.

The spectrum of NML Cyg shows structure at around 8.5, 11.5 and 12.7 μm. However, given the strong silicate absorption, it is difficult to determine where the 'true' continuum lies, and hence ascertain whether emission features are present. The *ISO* Short Wavelength Spectrometer observations of this source (Justtanont et al. 1996) should be very useful in this regard.

3.1 Comparison with h and χ Per

Summarizing the earlier discussion, we can say that of the 54 M supergiants in the present sample which are not associated with Per OB1, two stars (i.e. < 4 per cent of the sample) definitely show UIR-band emission. Adopting a generous estimate by including four of the doubtful UIR-band sources yields 11 per cent of the sample. In contrast, we found that five of 15 h and χ Per M supergiants in Paper 1 (33 per cent) are *definite* UIR-band emitters. Clearly, the h and χ Per M supergiants are significantly different from their counterparts in the rest of the Galaxy.

The basis for a possible explanation of this difference can found in the work of Lee (1970), who found that the h and χ Per supergiants have near-IR colours that are systematically bluer than those of normal Galactic M supergiants, and suggested that they are in a short-lived evolutionary phase, having already passed through a blue supergiant phase. This could change the elemental abundances at the stellar surface, which would in turn affect both the colours (via opacity effects) and the chemical composition of the outflow from which the dust condenses. All the h and χ Per stars with UIR-band emission have similar *K*-band fluxes, and hence (assuming that all are at the same distance) similar luminosities. The UIR-emitting supergiants could therefore be stars lying within a narrow mass range, and simultaneously passing through the same evolutionary

phase. If this phase is of short duration, only a small proportion of the stars in a broader sample with a more random age distribution (e.g. our present sample) will be passing through the particular phase that provides the combination of outflow chemistry and UV radiation necessary for UIR-band emission to arise.

4 MASS-LOSS RATES

The amount of mass lost by a massive star in the red supergiant phase has a critical effect on its subsequent evolution and final state (see e.g. Chiosi & Maeder 1986). The outflowing material is an important source of heavy elements for the interstellar medium (ISM). We have therefore estimated mass-loss rates for our rather large sample of M supergiants. Skinner & Whitmore (1988b) found a correlation between the mass-loss rate of M giants and supergiants, as determined from millimetre-wave CO emission, and the power emitted in the 10-μm silicate feature, and showed how this could be used to determine $\dot{M}$ for stars without CO measurements. The empirical relation was confirmed by the radiative-transfer dust envelope modelling of Hashimoto et al. (1990). We applied the Skinner & Whitmore (1988b) method to the present sample of supergiants (which includes 11 stars examined by SW). The power emitted in the silicate feature scales with the silicate strength parameter $B_{\rm sil}$, defined in the *IRAS* Explanatory Supplement as

$$B_{\rm sil} = 10[\ln f_{9.8\mu{\rm m}} - (0.589 \ln f_{7.9\mu{\rm m}} + 0.411 \ln f_{13.3\mu{\rm m}})],$$

where $f_{9.8\mu{\rm m}}$, $f_{7.9\mu{\rm m}}$ and $f_{13.3\mu{\rm m}}$ are the fluxes (in Jy) at those wavelengths.

Skinner & Whitmore took values of $B_{\rm sil}$ from the *IRAS* LRS catalogue, where the value for each source is expressed as a single digit. This, together with the fact that different instruments were used, leads to systematic differences between $B_{\rm sil}$ values derived from CGS3 and LRS spectra. To allow us to use the Skinner & Whitmore (1988b) calibration of $\dot{M}$ versus silicate emission, we compared the $B_{\rm sil}$ values derived from the LRS and CGS3 spectra. Linear regression for a set of 13 sources showed that the relationship

$$B'_{\rm sil} = -0.4 + 0.85 B^{\rm CGS3}_{\rm sil}$$

can be used to convert a CGS3-derived value of $B_{\rm sil}$ into a quantity $B'_{\rm sil}$ that closely approximates the LRS-derived value. We then applied the Skinner & Whitmore (1988b) method to these recalibrated values. Note that the $B_{\rm sil}$ values presented in Table 1 are as measured from the CGS3 spectra, not recalibrated to the LRS scale.

The power emitted in the silicate feature can then be expressed as $P_{\rm sil} = B_{\rm sil} F_{12} d_\star^2$, where F_{12} is the *IRAS* 12-μm flux in Jy, and $d_\star$ is the distance to the star in pc. The mass-loss rate, according to Skinner & Whitmore (1988b), is then simply $M = 4 \times 10^{-15} P_{\rm sil}$.

The mass-loss rates and adopted distances are listed in Table 1. The distances are mostly taken from Lee (1970), Humphreys (1978) and Garmany & Stencel (1992). Spectral types are taken from Lee (1970), White & Wing (1978), Ridgeway et al. (1986) and Jura & Kleinmann (1990). Where no published distance was available, we estimated the distance using spectroscopic parallaxes, adopting the calibrations of Schmidt-Kaler (1982). The stars for which spectroscopic parallaxes were used are V540 Sgr, BD+47 485, CIT11, HR 6693, IRC+40 427, IRC−20 429, HD 166105 and IRC−20 565.

For a number of our sources, we give only an upper limit for $\dot{M}$ in Table 1. These are sources where the value of $B'_{\rm sil}$ was zero or negative. This can occur when the observed spectrum shows featureless blackbody emission. A 3200-K blackbody, typical of photospheric emission from an M supergiant, would give $B^{\rm CGS3}_{\rm sil} = 0.09$ and hence $B'_{\rm sil} = -0.3$. Very weak silicate emission, where the silicate contribution at 13.3 μm is comparable to that at 9.8 μm, can also give rise to zero or negative values of $B'_{\rm sil}$. To estimate the upper limits for the mass-loss rate, we simply adopted 0.3 as the upper limit on $B'_{\rm sil}$. NML Cyg shows silicate absorption, and so the SW method is not applicable for this object.

Skinner & Whitmore (1988a) found a very high mass-loss rate of 4.3×10^{-4} $M_\odot$ yr^{-1} for AH Sco. We find a similarly high value, 4.5×10^{-4} $M_\odot$ yr^{-1}. AH Sco is the brightest star in our sample at 12 μm, and yet is one of the most distant, at 4.6 kpc (Humphreys & Ney 1974). These combine with the large value of $B_{\rm sil}$ to give a high mass-loss rate. If the star is at smaller distance, the mass-loss rate would be somewhat reduced: for instance, if AH Sco lies at 2 kpc, the mass-loss rate would be 8.5×10^{-5} $M_\odot$ yr^{-1}, still the largest in our sample, and considerably larger than the 1.4×10^{-6} $M_\odot$ yr^{-1} estimated by Hagen, Stencel & Dickinson (1983) from optical spectroscopy. Gehrz & Woolf (1971) obtained mass-loss rates for seven of the stars in our sample; their values are systematically lower than ours, with the average difference being 0.7 dex. Jura & Kleinmann (1990) estimated mass-loss rates for M supergiants within 2.5 kpc of the Sun, including eight for which we have $\dot{M}$ estimates either from the present sample or from Paper 1. Again, our values are generally higher by almost 1 dex (except for the case of α Ori, where we have good agreement). This illustrates the difficulty of obtaining accurate mass-loss rates for these stars. It is not clear which method best represents the true mass-loss rate; indeed observations at different wavelengths sample different portions of the circumstellar envelope, and hence are sensitive to the mass-loss rates at different epochs in the history of these stars (see e.g. Habing 1996 for a review of mass-loss rates for evolved stars).

What relationship is there between the dust emission properties and the photospheres of the stars? Fig. 4 plots the silicate feature strength parameter $B_{\rm sil}$ versus the M spectral subtype (i.e. photospheric temperature), while Fig. 5 plots $B_{\rm sil}$ against the luminosity class. In both cases, only stars with White & Wing (1978) spectral types are shown, in order to achieve a homogeneous set of spectral classifications, and the h and χ Per M supergiants from Paper 1 are included to increase the sample size.

Both figures show a positive correlation, albeit with large amounts of scatter. Thus, later-type (cooler), more luminous stars

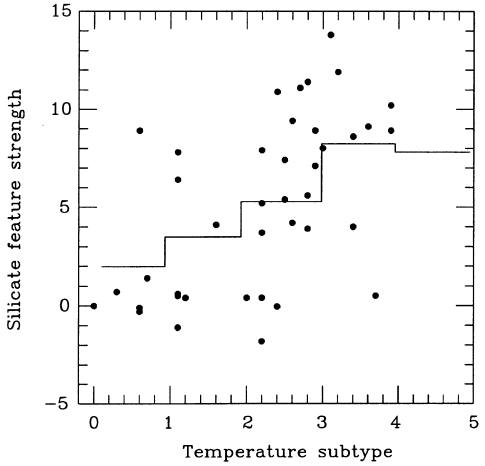

Figure 4. Silicate emission strength, $B_{\rm sil}$, as a function of M spectral subtype. Individual stars are shown as points, while the mean value for each subtype is plotted as a histogram.

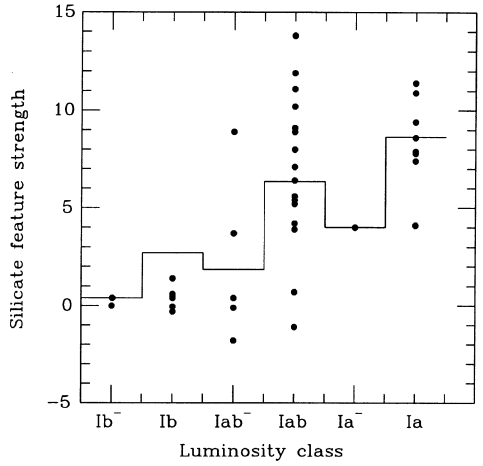

Figure 5. Silicate emission strength, $B_{\rm sil}$, as a function of luminosity class. Points: individual sources; histogram: mean values. Note that the means for classes Ib^- and Ia^- are based on only two and one points respectively.

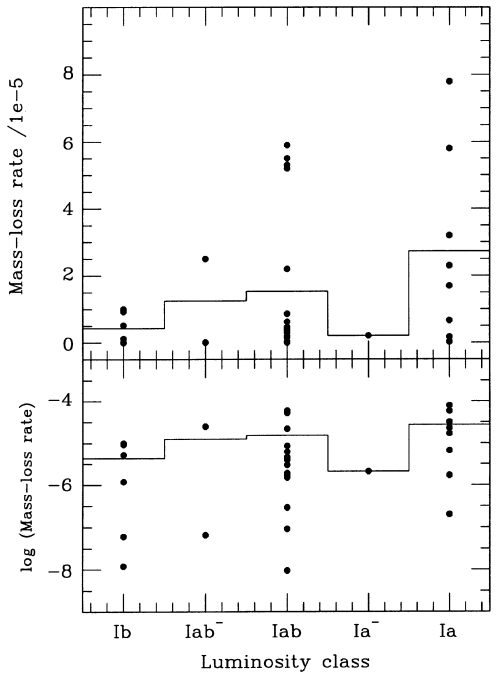

Figure 6. Mass-loss rate (in $M_\odot$ yr^{-1}) as a function of luminosity class. Points: individual sources; histogram: mean values. Stars with only upper limits for the mass-loss rate are excluded from this plot, while sources from Paper 1 are included. The means for classes Ia^- and Iab^- are based on only one and two points respectively. Upper panel: linear scale; lower panel: logarithmic scale.

tend to have higher-contrast silicate features, implying dustier envelopes, although there are stars with no detectable silicate emission for temperature classes as late as 3.7 and luminosity classes up to Iab.

Skinner & Whitmore (1988a) showed a strong correlation between $\dot{M}$ and stellar luminosity. However, in their formulation, both these quantities are dependent on the 12-μm flux and the square of the adopted distance. This means that errors in the distance could artificially strengthen the correlation, as they will displace points in a direction parallel to the apparent correlation. We therefore investigated the dependence of $\dot{M}$ on luminosity in an alternative fashion, using the luminosity classification of White & Wing (1978) as a distance-independent luminosity estimate. The absolute magnitude of a given luminosity class is likely to be independent of the temperature subtype for M supergiants (see e.g. Stothers 1972); this allows us to group all the stars of a given luminosity class into a single bin. Plotting mass-loss rate against luminosity class (see Fig. 6) results in a much less impressive correlation than that obtained by SW. The upper envelope of the distribution of data and the mean values both increase with luminosity class, but there is substantial scatter, especially when the mass-loss rates are plotted on a logarithmic scale. This large dispersion suggests that the weak upward trend of the mean values is not significant statistically.

Several factors could contribute to the looser correlation that we find, compared to fig. 3 of SW. We have already mentioned the effect of errors in the distances. Furthermore, the luminosity class of an M supergiant may not be a perfect measure of its actual luminosity. In fact, for the h and χ Per supergiants (which are all at approximately the same distance), the brighter, and hence more luminous, stars are not in higher luminosity classes than the fainter stars. However, Fig. 6 does still lend some support to the finding of SW that mass-loss rate increases with luminosity. The h and χ Per stars in Paper 1 are all thought to lie at the same distance, which allows relative comparisons between $\dot{M}$ and luminosity to be made. Table 1 of Paper 1 shows a very strong dependence of $\dot{M}$ on K, and hence on luminosity, if we accept the K-band flux as a measure of luminosity.

All of the stars in our h and χ Per sample with mass-loss rates between 2×10^{-7} and 1.3×10^{-6} $M_\odot$ yr^{-1} showed UIR bands (Paper 1). In our present sample, only two stars, AZ Cep and NS Vul, lie in this range. Neither of them appear to show UIR bands, so we can conclude that presence of UIR bands is not a universal property of M supergiants in this mass-loss range.

A broader range of mass loss rates, from 1×10^{-7} to 2×10^{-6} $M_\odot\,yr^{-1}$, includes eight stars in the new sample: AZ Cep, GP Cas, NS Vul, ST Cep, UW Aql, V717 Cyg, V1749 Cyg and IRC-10 419. V1749 Cyg and UW Aql are the stars in the present sample that most clearly show the UIR bands. We note that three of these stars are among those whose spectra suggested the presence of UIR bands, but were not of sufficient quality to allow a firm detection. For IRC+40 427, the other star in our sample that clearly shows UIR bands, we have only an upper limit of 6.3×10^{-8} $M_\odot$ yr^{-1} for the mass-loss rate. This is because it displays only a weak excess above the photosphere at 9.8 μm, while at 13.3 μm the silicate emission still makes a contribution to the total flux. The occurrence of UIR-band emission in M supergiants, therefore, depends not only on the mass-loss rate of the star, but also on some still-unknown combination of other factors.

In Paper 1 we suggested that the stars with large mass-loss rates could be emitting in the UIR bands at some level, but that the very strong silicate features of these stars drown out the bands in the observed spectra. Higher-resolution mid-IR spectra may help to separate narrow bands from a strong silicate 'continuum'. Table 1 also includes the peak wavelength ($\lambda_{\rm peak}$) and the FWHM of the silicate features. These were measured from the CGS3 spectra after subtracting blackbodies set to the effective temperatures of the stars, and normalized to the observed spectrum at approximately 8 μm.

Sloan & Price (1995) defined a silicate emission (SE) sequence based on ratios of the fluxes at 10, 11 and 12 μm of continuum-subtracted *IRAS* LRS spectra. They divided the sequence into eight classes, with objects in class SE1 having the broadest silicate

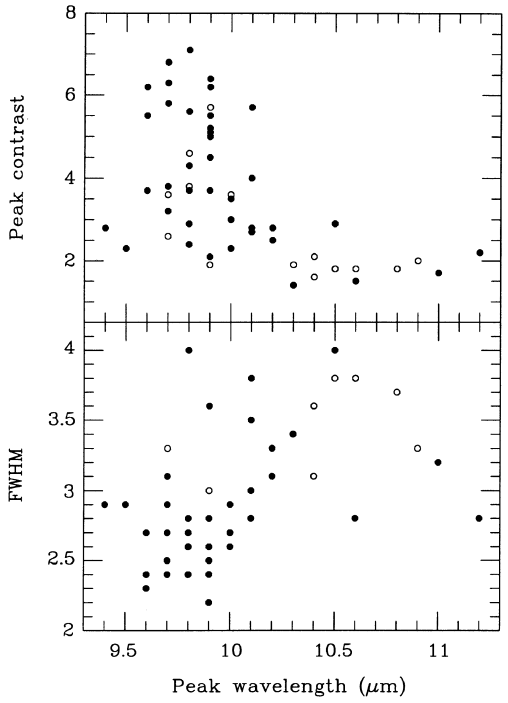

Figure 7. Silicate peak contrast $F_{obs}(\lambda_{peak})/F_{BB}(\lambda_{peak})$ (upper panel) and FWHM of the silicate feature (lower panel) as a function of peak wavelength. Open circles: stars from Paper 1; filled circles: the present sample.

features and SE8 the narrowest. Making equivalent measurements on a subset of our M supergiant CGS3 spectra with silicate emission, we find that they all lie in the locus of points found by Sloan & Price, and cover the whole range of SE classes. As expected, there is a correlation between our measured FWHM of the silicate feature and the SE class, with the spectra with smaller FWHM occupying the higher-numbered classes and vice versa. The UIR-emitting stars of the present sample and of Paper 1 lie in the lower and middle parts of the Sloan & Price range, with V1749 Cyg and UW Aql being in class SE5, IRC+40 427 in SE1, and the Paper 1 UIR emitters covering the range SE2–5. In terms of the Little-Marenin & Little (1990) classifications (which correlate well with the Sloan & Price classes), our sources cover the full range of Sil, Sil+, Sil++ and Broad classes.

The silicate features of our h and χ Per sources were divided in Paper 1 into two distinct groups, based on the peak wavelength and shape of the silicate feature. The IR-brighter stars had silicate features that peaked at 9.7–10.0 μm, with FWHM of 2.4–2.7 μm. UIR-band emission was not detected in any of these stars. The fainter stars (*IRAS* 12-μm flux <21 Jy) had peak wavelengths of 10.3–10.9 μm, and FWHM of 3.0–3.9 μm. Seven of these 10 stars clearly showed UIR-band emission, while for the remaining three (which were the faintest stars in the sample) it was difficult to discern from our spectra whether UIR bands were present or not.

In the new sample, there are eight stars with silicate features that peak at or beyond 10.2 μm. Their silicate features have FWHM in the range 2.8–4 μm. This subset includes V1749 Cyg, UW Aql and IRC+40 427 i. e. all three of the new UIR-emitting sources. The incidence of UIR-band emission among the stars with $\lambda_{peak} > 10.2$ μm is lower for the stars in the present paper than for those in Paper 1, but the samples are too small for a precise comparison. It nevertheless appears that the relationship between the silicate feature profile and the presence of UIR band emission noted in h and χ Per holds to some degree for the field M supergiants. This may be a result of the unusual chemical conditions that give rise to emission from C-rich particles in M supergiant envelopes also affecting the composition and/or structure of the silicate grains, and hence giving rise to changes in the peak wavelength and shape of the silicate feature.

Other trends are also apparent in our data. Table 1 shows that the stars with the largest values of B_{sil} have silicate features that peak at short wavelengths. There could be a systematic effect in this correlation, because the definition of B_{sil} assumes that the silicate feature peaks at 9.8 μm, so a feature with the same equivalent width but a longer peak wavelength would give a lower value of B_{sil}. We therefore measured the contrast in the silicate feature at the peak wavelength i. e. $F_{obs}(\lambda_{peak})/F_{BB}(\lambda_{peak})$, for all of our stars, and compared these values with λ_{peak}. The results are presented in Table 1 and Fig. 7, which shows a clear correlation. Fig. 7 also plots the FWHM of the silicate feature against the peak wavelength, and allows the two groups of stars mentioned above to be distinguished. The majority of our sample are in the first group, with $\lambda_{peak} < 10.2$ μm, while the stars with longer λ_{peak} have broader silicate features, and are not as tightly clustered in λ_{peak} or FWHM. The derived mass-loss rates for stars in the first group tend to be higher than for the stars in the second group, although the variations within both groups are large (more than two orders of magnitude). Both the Paper 1 stars and the field supergiants show broadly the same behaviour; there is clearly a range of silicate feature profiles among M supergiants, indicating a variation of composition, structure, or size of the silicate grains. Further investigation is required in order to understand the unusual silicate and hydrocarbon features observed in M supergiants.

ACKNOWLEDGMENTS

The United Kingdom Infrared Telescope is operated by the Joint Astronomy Centre on behalf of the UK Particle Physics and Astronomy Research Council. This research has made use of the SIMBAD database maintained by the CDS, Strasbourg. We thank the referee, Dr M. Cohen, for his useful comments.

REFERENCES

Allamandola L. J., Tielens A. G. G. M., Barker J. R., 1989, ApJS, 71, 733
Beck H. K. B., Gail H.-P., Henkel R., Sedlmayr E., 1992, A&A, 265, 626
Bester M., Danchi W. C., Hale D., Townes C. H., Delgiacomi C. G., Mékarnia D., Geballe T. R., 1996, ApJ, 463, 336
Chiosi C., Maeder A., 1986, ARA&A, 24, 329
Cohen M., Davies J. K., 1995, MNRAS, 276, 715
Cohen M., Walker R. G., Witteborn F. C., 1992, AJ, 104, 2030
Garmany C. D., Stencel R. E., 1992, A&AS, 94, 211
Gehrz R. D., Woolf N. J., 1971, ApJ, 165, 285
Gilman R. C., 1969, ApJ, 155, L185
Habing H. J., 1996, A&AR, 7, 97
Hagen W., Stencel R. E., Dickinson D. F., 1983, ApJ, 274, 286
Hashimoto O., Nakada Y., Onaka T., Tanabé T., Kamijo F., 1990, A&A, 227, 465
Humphreys R. M., 1970, AJ, 75, 602
Humphreys R. M., 1978, ApJS, 38, 309
Humphreys R. M., Ney E. P., 1974, ApJ, 194, 623
Jura M., Kleinmann S. G., 1990, ApJS, 73, 769
Justtanont K. et al., 1996, A&A, 315, L217
Kwok S., Chan S. J., 1993, AJ, 106, 2140
Lee T. A., 1970, ApJ, 162, 217
Little-Marenin I. R., Little S. J., 1990, AJ, 99, 1173
Lloyd Evans T., 1990, MNRAS, 243, 336
Monnier J. D., Geballe T. R., Danchi W. C., 1998, ApJ, 502, 833

Ridgway S. T., Joyce R. R., Connors D., Pipher J. L., Dainty C., 1986, ApJ, 302, 662
Rinsland C. P., Wing R. F., 1982, ApJ, 262, 201
Schmidt-Kaler Th., 1982, in Schaifers K., Voigt H. H., eds, Landolt-Börnstein, Numerical Data and Functional Relationships in Science and Technology, Group VI, Astronomy, Astrophysics and Space Research, Vol. 2b. Springer-Verlag, Berlin, p. 14
Skinner C. J., Whitmore B., 1988a, MNRAS, 235, 603 (SW)
Skinner C. J., Whitmore B., 1988b, MNRAS, 231, 169
Skinner C. J., Griffin I., Whitmore B., 1990, MNRAS, 243, 78
Sloan G. C., Price S. D., 1995, ApJ, 451, 758
Sloan G. C., Grasdalen G. L., LeVan P. D., 1993, ApJ, 404, 328
Stothers R., 1972, PASP, 84, 373
Sylvester R. J., Barlow M. J., Skinner C. J., 1994, MNRAS, 266, 640 (Paper 1)
Treffers R., Cohen M., 1974, ApJ, 188, 545
Waters L. B. F. M. et al., 1996, A&A, 315, L361
White N. M., Wing R. F., 1978, ApJ, 222, 209
Willems F. J., de Jong T., 1986, ApJ, 309, L39

This paper has been typeset from a $\TeX$/$\LaTeX$ file prepared by the author.